

**An Engineering Model of Woven Composites  
Based on Micromechanics**

*W.C. Carter, B.N. Cox, M.S. Dadkhah, W.L. Morris*

Rockwell International Science Center  
1049 Camino Dos Rios  
Thousand Oaks, CA

513-24

51296

### INTRODUCTION

Composites with three-dimensional woven architectures exhibit large strains to failure when compared to composites made up of the same materials but not with three-dimensional interlocking tows. The fracture mechanics of such three-dimensional architectures is a subject requiring substantial investigation and experimental testing.

Classical fracture mechanics concepts (for instance, an isolated defect in a homogeneous body) will not be applicable to the woven fracture test specimen. The use of an isolated singularity to characterize an entire specimen is inadequate when the density of defects is considerable and the material is heterogeneous. Modelling of such a complex system requires a great deal of insight and consideration as well as prudent choices of model sizes to make numerical schemes feasible.

The purpose of this manuscript is to review our recently acquired knowledge of damage accumulation in woven composites and to describe a practicable model of the macroscopic behavior in these and other complex composite architectures based on such knowledge. In this manuscript, discussion will be limited to uniaxial compressive loading; considerations of general loading (monotonic and cyclic) will appear in a subsequent manuscript.

Our modelling efforts may be briefly described as follows: the composite is subdivided into microstructural elements (*microelements*) in which the micromechanical modelling is either understood rigorously or can be represented adequately by statistical parameters. There can be microstructural elements for many different types of composite components, such as the various types of warp and weft and matrix for three-dimensional woven composites. The physical dimensions of microelements are made as large as possible while the response within the element can still be represented by a single micromechanical calculation. The various elements are linked together (sometimes by associating distinct corners and edges, sometimes by superposition) in a pattern which resembles a particular weave architecture (Fig. 1). The model can then be loaded in any manner and the linear and non-linear elastic responses of representative weaves can be calculated. After the elastic regime, the fracture response is determined by monitoring the damage accumulation.

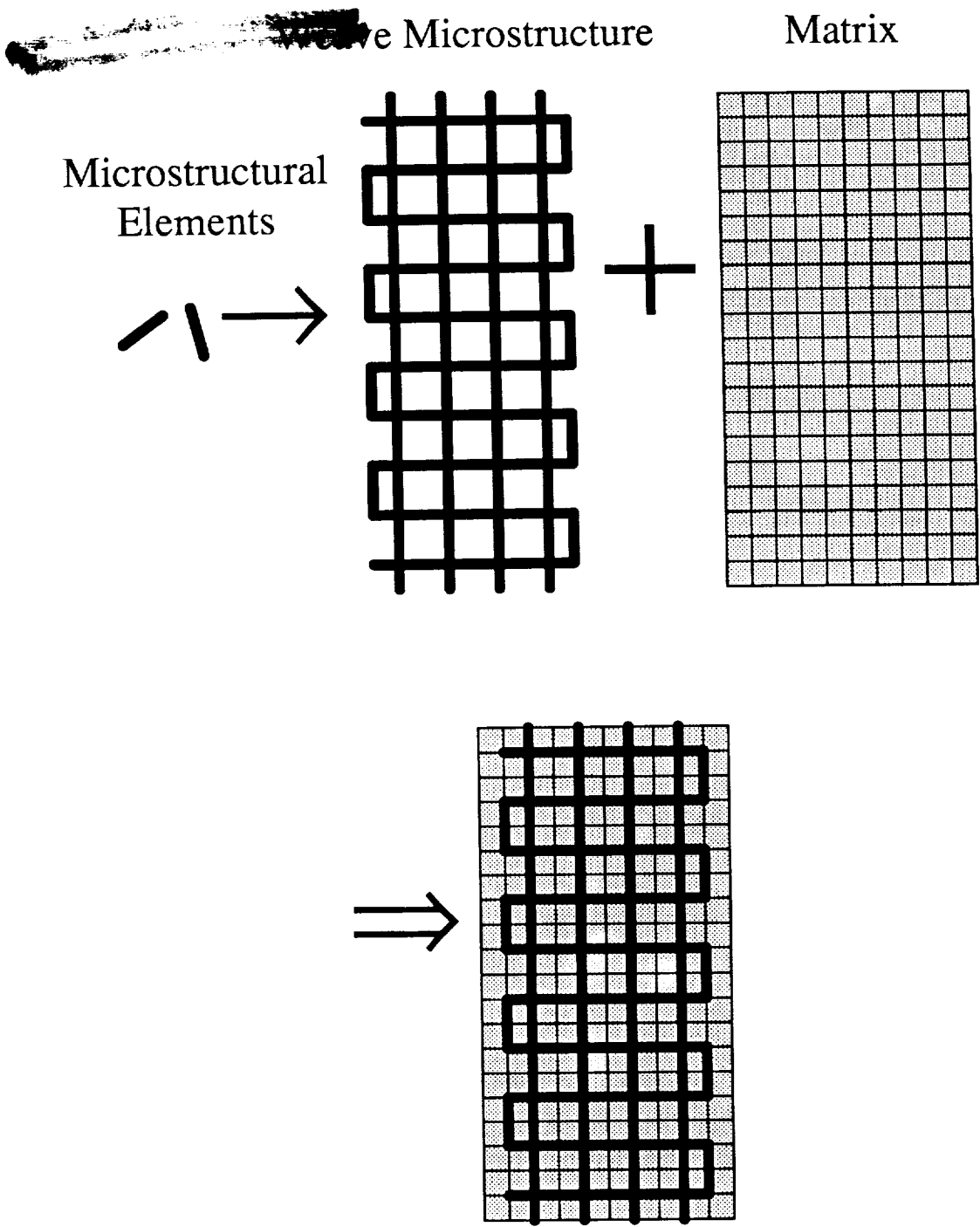


**Figure 1: Illustration of Micro-element Model**

Microstructural elements are designed to mimic derived micromechanical results; in the case shown, the microelements duplicate the derived response of kinking (on compression) or rupturing (tension) tows which are embedded in an elastic matrix. The microelements are assembled into an architecture which mimics that of a particular composite, in this case an ideal (two-dimensional) through-thickness orthogonal interlock weave. The architecture is then embedded into a matrix which has micromechanical behavior of its own and the model is loaded. Initial fracture can be predicted and damage accumulation can be monitored.

## BACKGROUND

The nature of the *local* failures in the three-dimensional woven composites is similar to those observed in other fibrous composites. For the case of uniaxial compressive loading, possible local failure mechanisms are listed below; not all of these mechanisms have been experimentally observed.

- 1 *Buckling* The entire specimen may fail macroscopically by classical Euler buckling; this is determined by component geometry and design and does not fall under the subject micromechanics since it is a material failure. Localized buckling of tows does occur either with or without matrix-fiber delamination discussed below.
- 2 *Matrix Failure* The matrix may fail along plains of maximum shear. Intact tows will act as bridging mechanisms for mode-II matrix cracks which will typically lie along planes oriented at 45° to the loading axis.
- 3 *Fiber Crushing* If the compressive strength is exceeded in the tows whilst being supported by an intact matrix, the fibers may fail with no out-of-plane displacement. The crushing strength of the tows is expected to follow weak-link statistics.
- 4 *Fiber Kinking* In kinking, a segment of a tow rotates away from the loading axis as a rigid body and the tow is ruptured along parallel planes (Fig. 2). The tow loses its load bearing capacity at the kink; but, if the matrix is still intact, stresses will build back up in the tow as stress is transferred back to the fiber over a characteristic distance called the shear transfer length. The micromechanical conditions for kinking are known [1, 2, 3]. The critical axial stress,  $\sigma_c$ , for kinking is:

$$\sigma_c = \frac{k^* - \tau^\infty}{\phi_{total}} \quad (1)$$

where  $k^*$  is related to the matrix yield stress,  $\tau^\infty$  is the remote shear loading, and  $\phi_{total}$  is the total tow misalignment away from the load axis. Significantly lower critical kinking stresses occur in segments of tows which are misaligned. The effect of fiber misalignment in two-dimensional woven composites has been observed [4].

Interactions between tows can also lead to the formation of kink bands. Such a case is illustrated in Fig. 3 where a warp weaver pushes a filler (weft) against a stuffer (straight warp). The additional contact load has the effect of increasing the magnitude of the shear at the tow and knocks down the critical kinking stress as in Eq. 1.

- 5 *Delamination* Delamination of the tow-matrix interface is a possible, but not a necessary, precursor to kinking. If delamination occurs over a sufficient length of a tow, then the loss of constraint will allow the tow to rotate freely into greater misalignment—thus knocking down the kinking critical stress. Delamination may also occur as a result of a fiber kinking in a previously un-delaminated region.

Fiber kinking has been observed in many composite systems: carbon-carbon composites [5], glass fiber-epoxy matrix [6], aligned carbon fiber-polymer composites [7], [4], carbon, and glass fiber-epoxy matrix [8]. The micromechanical models leading to Eq. 1 [2] are applicable in each case.

SC53780  
SC53600

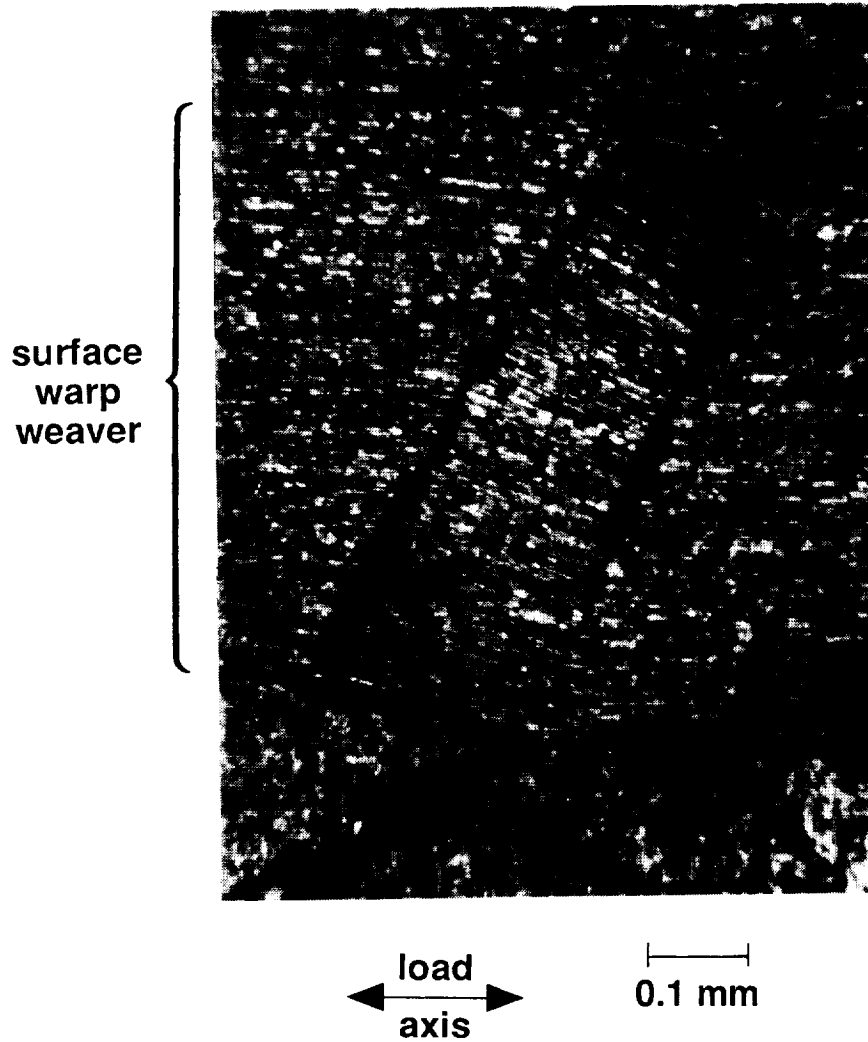


**Figure 2: Kink Band Failure in Compression**  
Layer-to-layer angle interlock – AS4/Tactix 138-H41

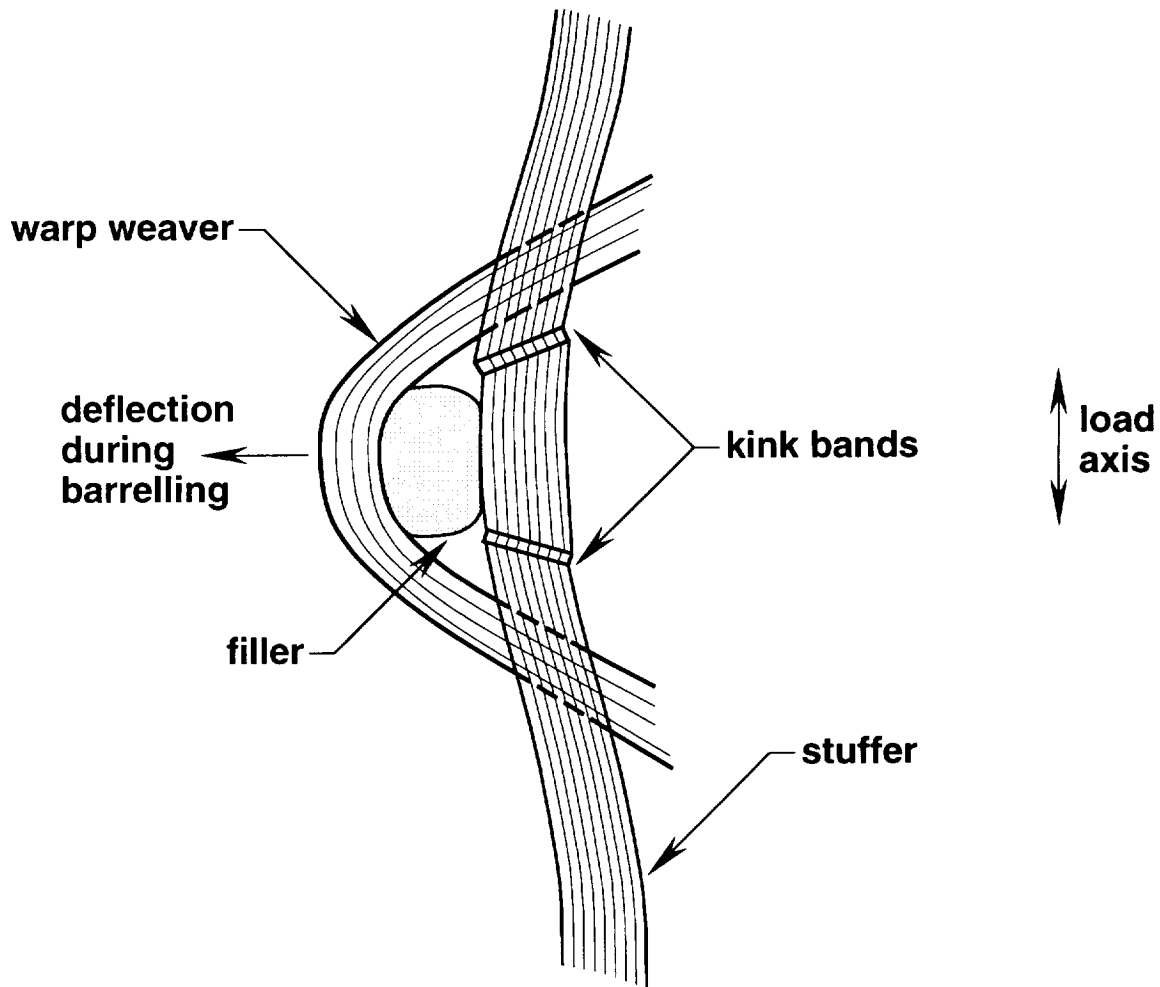


**Figure 3: Illustration of Contact Between Tows**

Modelling must incorporate interactions between various parts of the structure. This illustrates a kink band which has formed when a warp weaver pushed a filler against a stuffer.

## EXPERIMENTAL OBSERVATIONS IN 3D WOVEN COMPOSITES

Results of several monotonic compression tests are illustrated in Fig. 4. Experimental techniques and specimen preparation may be found in a previous publication [8]. All of the weave architectures show considerable ductility after the initial load drop. Yield strengths are typically 150-200 MPa with yield strains of 0.5%. Typical strains to failure are 5-12%.

At the initial yield, damage appears at the specimen surface as tows which have buckled and kinked out of the interface where the constraint is lowest. Sectioning of a just-yielded specimen did not show any fiber failures or delaminations in the specimen interior: all initial failures are correlated with the lack of tow constraint at the specimen surfaces.

Sectioning of specimens which have undergone some plastic loading (here, plasticity refers to the load-displacement diagram, not to the physical process of deformation) revealed kinks adjacent to small delamination cracks. In the interior of the specimen, the locations of the kinks appear to be spatially uncorrelated. Kinks observed near the specimen surface are either uncorrelated with any previous damage or they appear where a delamination crack veers from the surface into the matrix and terminate at a kink site.

At later stages of plasticity, kink failures become spatially correlated and link up via delamination cracks which veer into the matrix and intersect one another. Several such growing defects begin to link together along a shear band at 2-4% strain. Subsequently, deformation becomes localized to the shear band with intact tows providing mode-II bridging tractions. Final failure occurs when the tows can no longer provide sufficient bridging.

## MACROSCOPIC MODEL BASED ON MICROSTRUCTURAL ELEMENTS

The composite architecture is subdivided into regions, each of which is to be represented by a particular micromechanical model or by an appropriate statistical model. Such regions become *microelements* which will implicitly represent an averaged mechanical behavior. The microelement need not have the same measure as the region to which it is applied; in the woven materials for instance, a one dimensional object (i.e., a geometric length,  $L_s$ ) with six degrees of freedom (displacements and rotations) at each of its two nodes represents the volume in a tow segment of length  $L_s$ . With the understanding that the model need not be elastic or even plastic in the conventional sense, such a one-dimensional element can be called a beam. The beams can be assembled together and superimposed into a three-dimensional network of brick elements which represent the micromechanical behavior of the matrix. Because the elements are linked together at nodes, only the *average* behavior of the representative region is probed. This provides a practical way of realistically modelling fracture and damage in a complicated composite architecture; such averaged behavior is reasonable when applied to a micromechanical model. It may not be feasible to model the continuum mechanical behavior in a heterogeneous, geometrically disordered composite architecture. To summarize, the microelement model consists of three parts: 1) the micromechanical models, 2) the various types of representative elements, and 3) the geometry of the element connectivity.

Working models for fracture and damage accumulation in woven composites follow from the results of idealized micromechanical calculations. For instance, a segment of tow (over which the

angle interlock weaves

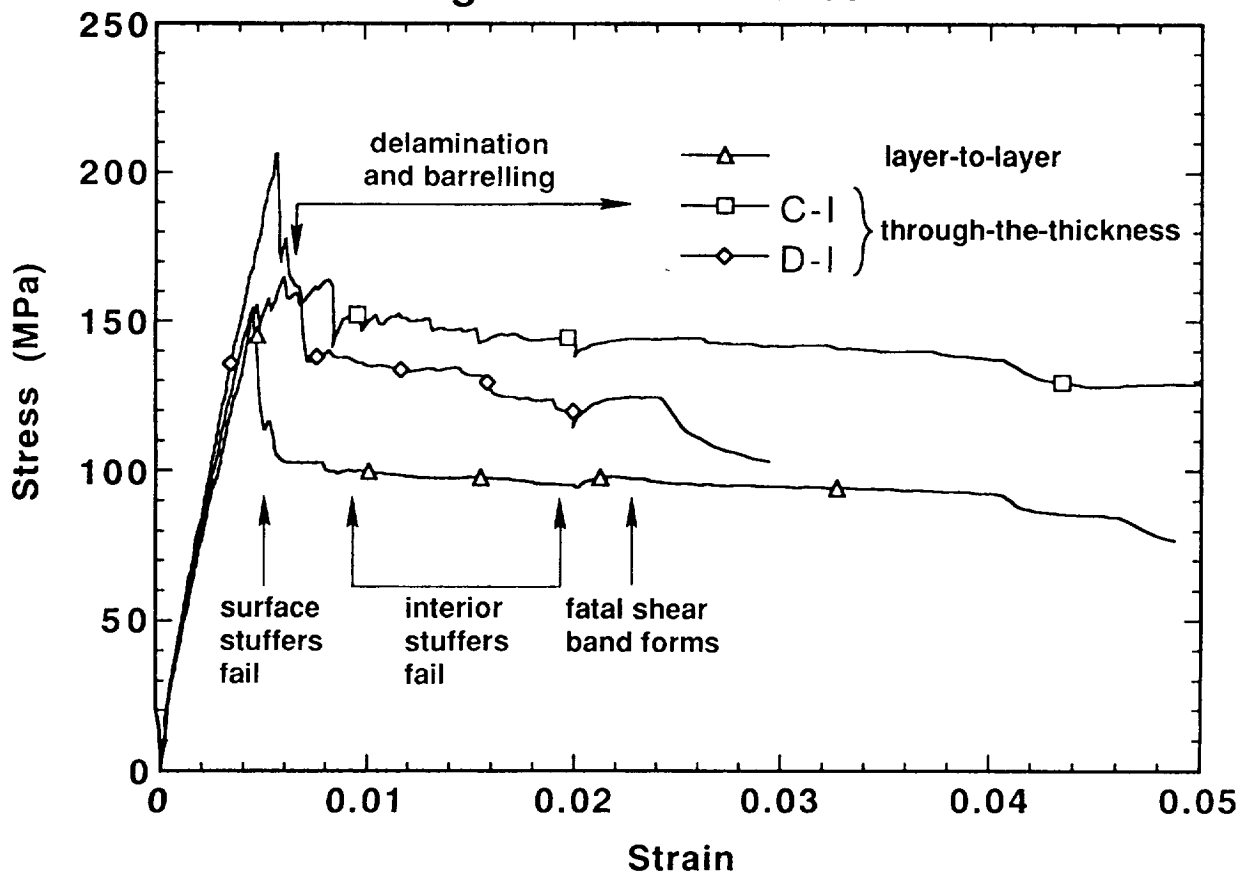


Figure 4: Monotonic Compression Dog-Bone Specimens

matrix stress transfer is changing slowly) may be considered an elastic flexural member until the condition for fracture (Eq. 1) is satisfied whereupon the tow's load bearing capacity drops significantly and the load is shed to the matrix. The matrix can be considered an effective anisotropic medium which can delaminate or fail depending on its immediate environment and stress. Every element is positioned in a manner which reflects the geometry of the composite (Fig. 1) and then the system is numerically loaded as desired.

Stochastic effects can be modelled in two distinct ways: 1) by picking critical microstructural flaw sizes (or, fracture strengths) according to some distribution, or 2) perturbing the coordinates of the element nodes about some idealized position (Fig. 5); in this way effects of tow waviness can be simulated. Monte Carlo simulations can be performed and design parameters such as the lower limit and variability of strength, or the distribution of the work of fracture can be assessed in terms of inherent material variability.

One major function of the model is to evaluate the failure mechanisms and damage accumulation as a function of composite architecture. The size scale of the element is picked to be the largest value over which the micromechanical models apply, or the scale over which large gradients in stress decay. A reasonable value of the element length scale for the woven composites is the shear transfer length,  $l_s$ :

$$\frac{l_s}{R_f} = \frac{\sigma_c}{2V_f \tau_y} \quad (2)$$

where  $\sigma_c$  is the interface delamination stress,  $V_f$  and  $R_f$  are the tow volume fraction and radius, and  $\tau_y$  is the matrix yield stress. The ratio  $l_s/R_f$  is approximately 10 for the woven composites illustrated in Fig. 4. Element length scales smaller than  $l_s$  should not affect the quality of the damage simulation, but larger element sizes will introduce an artificial scaling. In practice, scales are picked to be less than  $l_s$ , but large enough to result in a relatively small number of elements. It should be reiterated that the purpose of the simulation technique is not to calculate approximations to the continuum stress and strain values; stresses and strains are calculated, but on a mesh which is typically more coarse than used in other finite element methods.

The results of the simulation which we will show below were obtained through the use of a commercial solver (ABAQUS) but the method could be used—in principle—with any finite element code routine. The method is a hybrid finite element technique and the idea of superimposing elements has been utilized before in studies of the elastomechanics of reinforcement structures (e.g., strut and frame structures on a fuselage). The idea of using microstructural fracture mechanics for elements to model the accumulation of damage has been suggested previously [9]. Methods of arranging the microelements to mimic the composite architecture continue to be investigated carefully.

## MODELLING RESULTS

Modelling is still in progress in two and three dimensions for a variety of different microstructural elements. Some of the initial results appear below; even more promising results are being obtained at the writing of this manuscript.

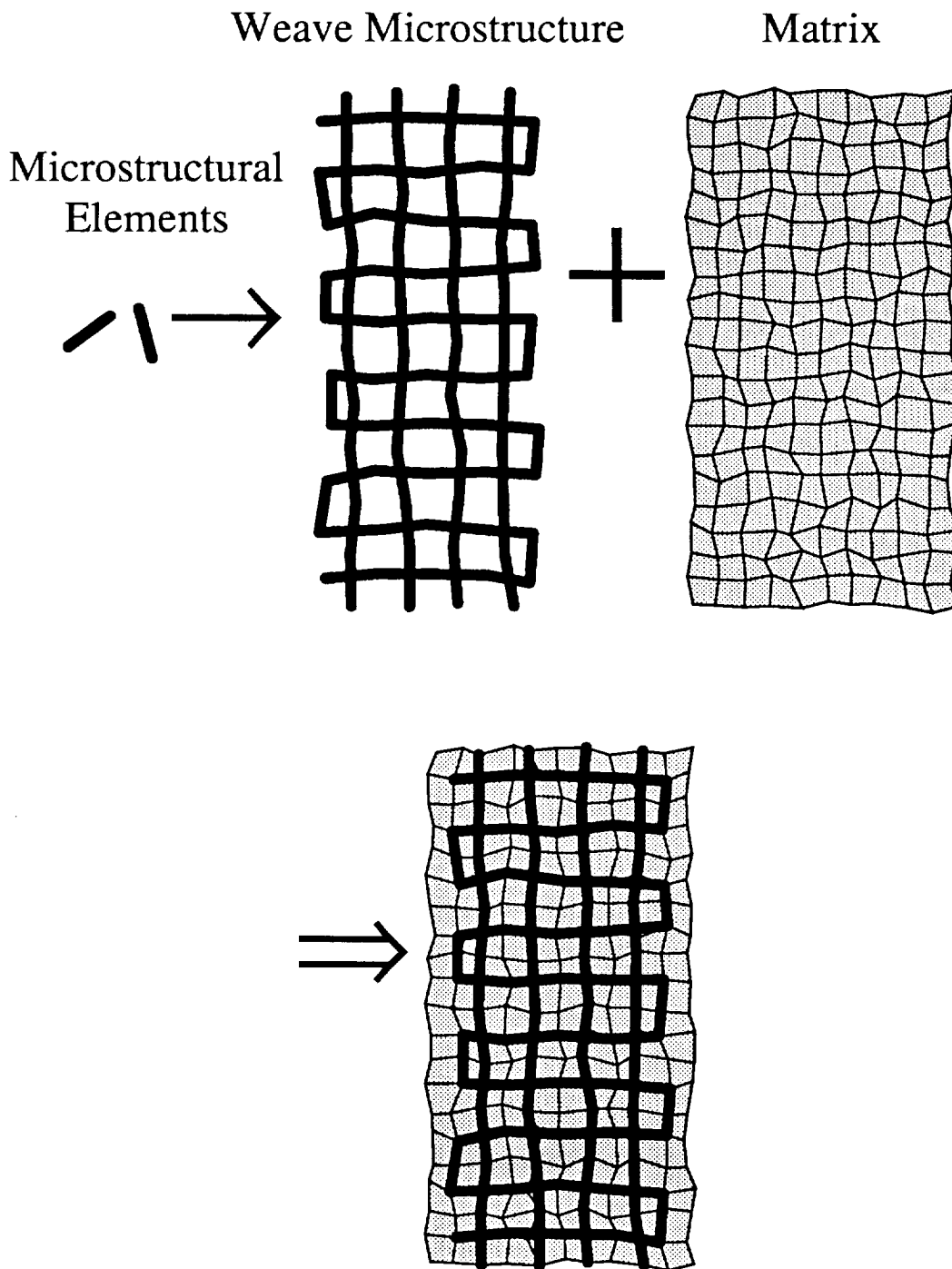


**Figure 5: Illustration of Perturbed Geometry in Micro-element Model**

Effects of inhomogeneity due to tow waviness can be modelled by perturbing the geometry of the model as in the above illustration. The size of the perturbation can be varied and arbitrary spatial correlations may be introduced. This is one of two ways statistical variations can be introduced; distributions of parameters, such as strength, can also be imposed on the microelements taken individually.

Results from two simulations appear in Figs. 6-7. The modelled geometry is a though-thickness orthogonal interlock weave, represented in two dimensions. The two models are identical in all respects save that the one in Fig. 7 has been geometrically perturbed to simulate the inevitable effects of processing variations on the weave architecture. The elastic stiffness of the tows is ten times that of the matrix. The matrix is fully elastic in Figs. 6-7 and the stuffers fail at a critical strain of 1%. In this particular simulation, the warp weavers are assumed not to fail. The warp weavers are connected to the stuffers where they cross and the weave architecture is embedded in four-noded matrix elements.

The model in Fig. 6 shows the load-displacement curve for the ideal geometry. The cartoons A-E illustrate the damage development in the tows at increasing values of strain. In cartoon B, the outer stuffers fail over most of their length, quickly followed by general failure of the interior stuffers. Since all stuffers have nearly the same load at failure and the matrix stresses are fairly homogeneous for this ideal geometry, all the stuffers fail at once, giving rise to a large load drop in the force-displacement diagram.

The model in Fig. 7 shows the results for a perturbed geometry (the scales are the same as in Fig. 6). The load displacement diagram shows the same qualitative behavior as the experimental curves in Fig. 4. Since all the of the stuffers do not fail together, stuffers fail at higher strains and thus the work of fracture is enhanced. However, the elastic stiffness for the perturbed geometry is slightly reduced and its strength is diminished.

Load-displacement curves for a slightly different model are illustrated in Fig. 8. In this case, the matrix has plastic behavior; and, for the diagram on the right of Fig. 8, the geometry is perturbed and the tow failure strengths have been uniformly distributed about an average strength. The loading behavior is very much like what is experimentally observed. *It is reasonable to conclude that the randomness and heterogeneity in the experimental specimens have a large influence on the mechanical behavior.*

## FUTURE WORK

Models for other weave architectures are being built and tested and results from those two and three dimensional stochastic models will appear in a future publication. Other microstructural elements are being developed, such as a delamination element between fibers and matrix. More realistic models for effective damage production in the matrix and orthotropic elastic behavior are being incorporated.

Monte Carlo type calculations will be made and statistical variations in the fracture response of the weave architectures will be obtained.

This technique is expected to find a wide range of applicability and utility in modelling composite architectures.

## ACKNOWLEDGEMENTS

This work is funded by NASA Langley Research Center under contract NAS1-18840, contract monitors C.C. Poe and C.E. Harris. We are grateful to Mike James for insightful discussions and assistance, and to Norman Fleck for critical discussions of the model and calculations.

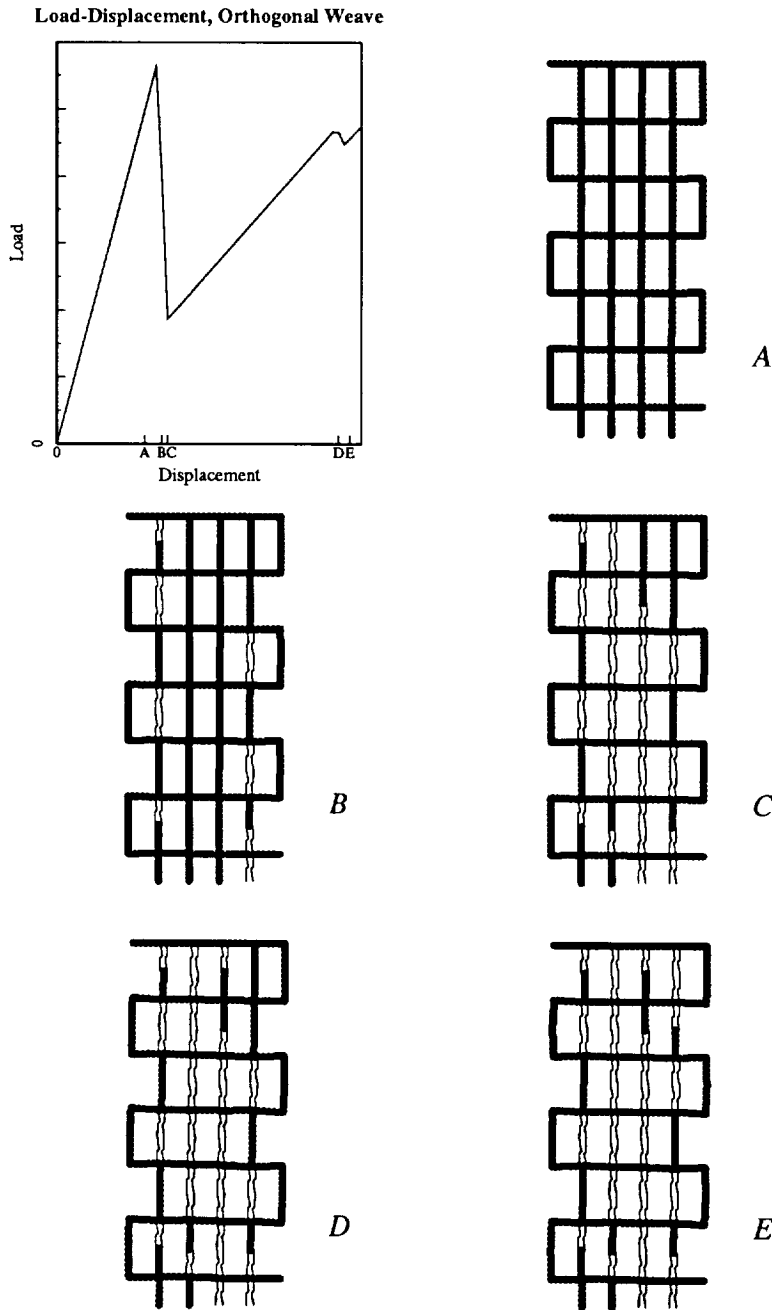


**Figure 6: Ideal Orthogonal Interlock Geometry**

This schematic shows the load-displacement behavior for an idealized plane of orthogonal interlock woven material. The results are obtained by a hybrid finite element technique described in the text. The tows are embedded in an elastic matrix which carries the load which is shed by a tow when it kinks (shown for illustration in outline). The orthogonal warp weavers are not allowed to fail in this particular model. The vertical tows (stuffers) have a failure strain of 0.01. The tows are 10 times stiffer than the matrix; the matrix is not illustrated.

Force-Displacement, Perturbed Geometry

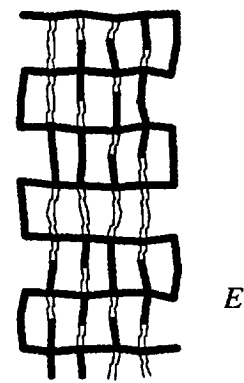
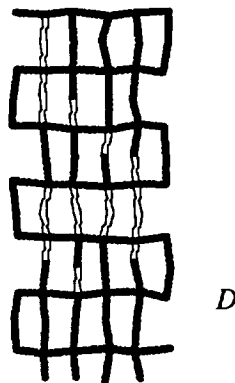
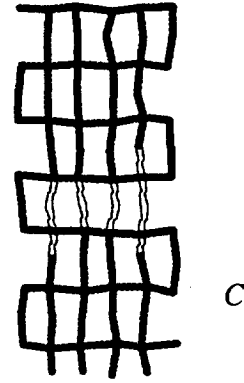
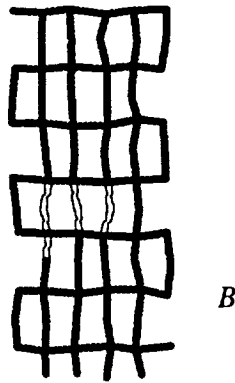
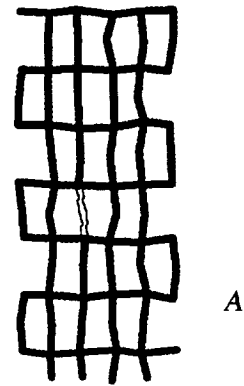
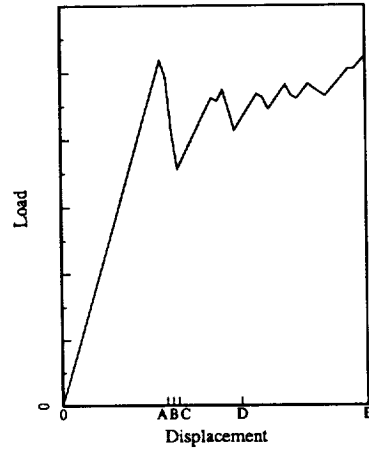
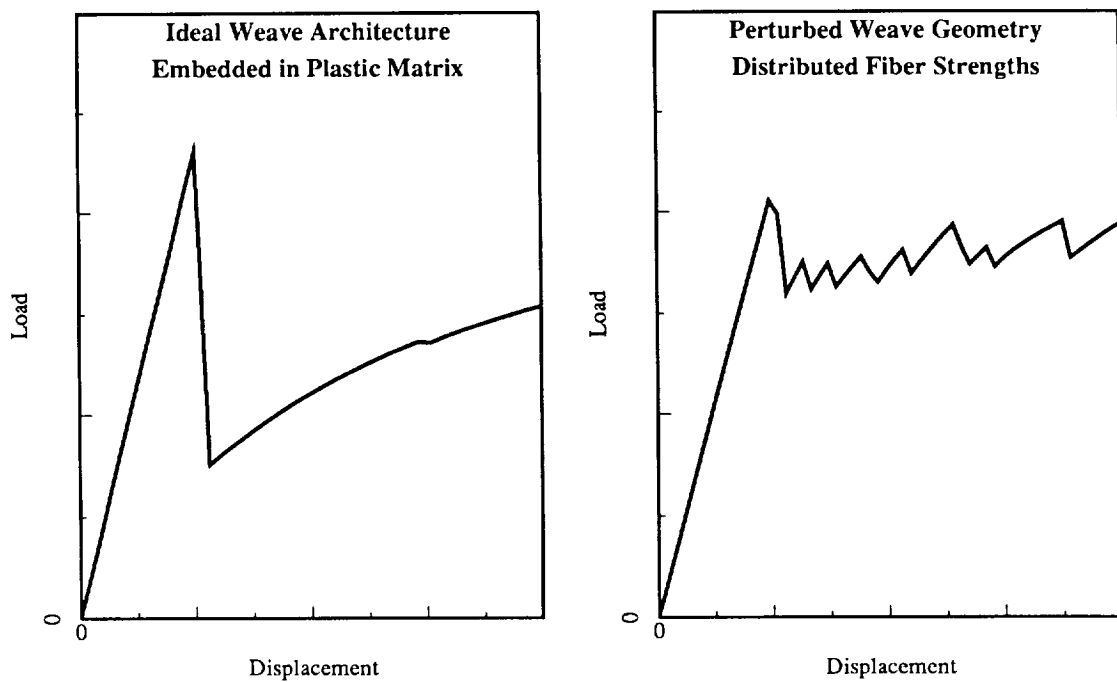


Figure 7: Perturbed Orthogonal Interlock Geometry

This shows the effect of introducing a realistic geometric distortion of the beam elements which represent the tows. The results are obtained by a hybrid finite element technique described in the text. Although the strength and stiffness of the perturbed structure are diminished, the work of fracture is distributed over a larger number of stuffers and the initial load drop is much less than for the ideal geometry.



**Figure 8: Results with Matrix Damage**

In this model, a plastic response is associated with matrix damage and included in the simulation. For the figure on the right, the distribution of fiber kinking stresses is included as well as a geometric perturbation. The load displacement curve is qualitatively similar to the experimentally observed curves.

## REFERENCES

1. Argon, A.S.: "Fracture of Composites," *Treatise of Materials Science and Technology*, Vol.1, Academic Press, New York, 1972.
2. Fleck, N.A.; and Budiansky, B.: "Compressive Failure of Fibre Composites" submitted to *J. Mat. Phys. Sols.*
3. Budiansky, B.: "Micromechanics," *Computers and Structures*, Vol. 16, pp. 3-12, 1983.
4. Reifsnider, K.L.; and Mirzadeh, F.: "Compressive Strength and Mode of Failure of 8H Celion 3000/PMR15 Woven Composite Material," *J. of Comp. Tech. and Res.* vol. 10, no. 4, pp.156-164, 1988.
5. Evans, A.G.; and Adler, W.F.: "Kinking as a Mode of Structural Degradation in Carbon Fiber Composites" *Acta Metall.* ol. 26, pp. 725-738, 1978.
6. Chaplin, C.R.: "Compressive Fracture in Unidirectional Glass-Reinforced Plastics," *J. Mater. Sci.*, vol. 12, pp. 347-352, 1977.
7. Parry, T.V.; and Wronski, A.S.: "Kinking and Compressive Failure in Uniaxially Aligned Carbon Fibre Composite Tested Under Superposed Hydrostatic Pressure," *J. Mat. Sci.* vol.17, pp. 893-900, 1982.
8. Cox, B.N. *et al.*: "Mechanisms of Compressive Failure in 3D Composites," Submitted to *Acta Met et Mat.*
9. K.L Reifsnider, K.L.: "Life Prediction in Advanced Material Systems," pp. 85-110, *Fatigue of Advanced Materials, Proc. of the Engin. Found. Int. Conf.*, R.O. Ritchie, R.H. Dauskardt, B.N. Cox Eds, MCEP Pub., U.K. 1991.